City, University of London Institutional Repository

A Method for Along-wind Vibration Control of Chimneys by Tuning Liners

Yusong Cheng[1], Kaoshan Dai[1,2,3*], Yangzhao Liu[1*], Han Yang[1], Mengran Sun[1], Zhenhua Huang[4], Alfredo Camara[5], and

Yexian Yin[6]

[1] Department of Civil Engineering, Sichuan University, Chengdu, 610065, China; [2]MOE Key Laboratory of Deep

Underground Science and Engineering, Chengdu, 610065, China; [3]Failure Mechanics & Engineering Disaster Prevention

and Mitigation, Key Laboratory of Sichuan Province, Sichuan University, Chengdu, 610065, China; [4]College of

Engineering, University of North Texas, Denton, Texas, US 76201; [5]Department of Civil Engineering, City, University of

London, London, EC1V 0HB, UK; [6]SEPCOIII Electric Power Construction Corporation, 882 Tong'an Rd, Qingdao,

261061, China. Corresponding authors: kdai@scu.edu.cn (Dai, K); liuyangzhao@scu.edu.cn (Liu, Y.)

Abstract: Reinforced concrete chimneys with steel liners are widely used in waste gas discharge of

industrial facilities, and guaranteeing their safety performance in harsh environments is important for

industries and society. This paper proposes a novel method for the reduction of along-wind vibration in

chimneys with liners by tuning the movement of the suspended liners to the response of the outer cylinder,

and the conventional rigid supporting platform is replaced by a combination of radial horizontal tuning

systems and vertical suspension systems. This 'tuned liners' method is applied to a simplified beam-like

model that is able to capture the liners/chimney interaction and is validated against a more detailed finite-

element shell model. A design method is proposed to obtain parameters of the tuning system that lead to

significant reduction of along-wind vibrations whilst satisfying the relative response requirement. A

comprehensive study of the structural vibration under stochastic wind actions is performed to

demonstrate the effectiveness of the proposed system. The characteristics of the relative vibration of the

outer cylinder and the liners are studied. Comparison with conventional TMD solution is conducted to

further explore the advantage of the tuned-liners system under stochastic wind actions. The results

indicate that the top displacement and acceleration of the outer cylinder is effectively reduced by 62%

and 70% with the tuned liners, respectively. A similar performance using a conventional TMD would

require an auxiliary vibrating mass that is approximately 300 tons, which is avoided with the proposed tuned liners. Results show that the proposed technique could be effective in the wind-induced control of chimneys in multiple directions, even with some unintentional eccentricities.

Keywords: chimneys, liners, tuning system, along-wind action, vibration control

1 Introduction

Reinforced concrete (RC) chimneys are essential industrial structures that play a key role in waste flue gases discharge of industrial facilities, such as different types of power plants. Chimneys are usually slender and flexible structures that are sensitive to external actions like wind [1] and ground motion [2]. They are prone to large deformations and vibrations that can induce damages [3] and result in reparation and downtime costs, or even collapse of the structure. A clear example was the collapse of a 140-m tall steel chimney due to the vortex-induced resonance [4].

Therefore, guaranteeing the structural safety of chimney structures under hazardous actions is very important for the economy and society [5]. To this end, the structural design of chimneys considering their dynamic response and potential damages under violent actions is an important process [6]. The most accurate way of studying the dynamic response of chimneys is by means of on-site measurements [7][8][9], but they cannot inform the structural design stage of chimneys that are not built yet, and they are difficult to conduct due to the height and stiffness of these structures. Wind tunnel testing emerged as an alternative approach to capture the dynamic characteristics of reduced-scaled chimney models, and it can address complex aerodynamic phenomena [10], However, wind tunnel testing can be expensive and time consuming, and therefore it is not always available. On the other hand, numerical analysis is an efficient way to simulate the dynamic response of chimneys and can consider the actual structural

and environmental features, for instance, the flexibility of soil under the foundation of chimneys [11][12]. Numerical modeling with finite element (FE) models is widely used by engineers and researchers for the dynamic analysis of chimneys [13]. In the FE models for dynamic response analysis, the chimney is usually considered as a cantilever beam, sometimes further simplified to a lumped mass model (Elias *et al.* [14], Zhang *et al.* [15], Qiu *et al.* [16], Wilson [2]). More accurate models have been proposed using shell and solid elements (Zhou *et al.* [17], Karaca *et al.* [18], Cheng *et al.* [19]). Longarini and Zucca [20] compared the FE models of a chimney with liners under ground motions using beam elements and solid elements, and they demonstrated that the differences were small when the chimney remains in the elastic range.

Apart from the analysis methods to study the dynamic response of chimneys, there is a large body of research focusing on the vibration control, particularly with tuning systems. Although different vibration reduction systems have been proposed for tall and flexible structures recently [21][22], the use of conventional tuned mass dampers (TMD) is still the most popular technique to control the wind-induced responses in chimney structures [23]. Brownjohn *et al.* [7] demonstrated the effectiveness of TMD in wind-induced vibration control of reinforced concrete chimneys based on the real-time monitoring data of a 183-m chimney equipped with a TMD at the top. Elias *et al.* [6][24] applied distributed multiple tuned mass dampers (d-MTMD) to control the along-wind vibration of a RC chimney and observed the favorable effect on the control of the contribution of multiple vibration-modes to the top displacement and acceleration. However, the use of tuned dampers requires the installation of large auxiliary non-structural masses or liquid tanks that add a significant weight and cost to the structure.

This study proposes a novel control method in which the tuned vibrational mass is provided by the liner itself without auxiliary mass required, and the conventional rigid supporting platform is replaced by a

combination of radial horizontal tuning systems and vertical suspension systems. In Section 2, a simplified numerical model of chimneys with liners is proposed; a typical chimney with liners is established using the simplified model and it is validated against a more detailed shell-like FE model. In Section 3, a series of four along-wind records is generated to analyze the dynamic response of the uncontrolled chimney using the simplified model. In Section 4, the tuned-liners method is introduced in detail and the corresponding simplified model is implemented; an optimization method is proposed for the tuned chimney considering turbulent wind actions and parameter optimization of a chimney is conducted as a case study. Section 5 demonstrates the effectiveness of the proposed solution by, comparing with conventional TMD solutions and analyzing the response in different directions. Finally, the safety of the proposed solution is demonstrated in Section 6 based on the analysis of the relative vibrations lateral opening restraints and unintentional eccentricities.

2 High-rise chimneys with liners

2.1 Main components and dimensions of a chimney

Chimneys with liners such as those used in thermal power plants usually consist of a RC outer cylinder, steel liners, supporting platforms and ancillary facilities. The RC outer cylinder is an important load-bearing structure of the chimney and it is the main element resisting wind and seismic loads. Steel liners can be divided into self-supported, fully suspended and sectionally suspended types. The fully suspended liners are usually preferred as they improve safety and maintenance by connecting with the RC outer cylinder through a supporting platform at the top and anti-sway platforms at certain positions along with their height.

In this work a typical high-rise chimney with two fully suspended liners is considered. The structure is

shown in **Fig. 1**-(a). It has a RC outer cylinder with a height of 216.5 m resting on a piled foundation. The outer diameter of the RC wall varies from 24 m at the base to 18.3 m at the top of the chimney. Two circular-section steel liners are introduced through orifices in the RC outer wall at 30 m from the base, and their top is 220 m above the base of the chimney. The outer cylinder and the liners are connected by the supporting platform at the elevation of 205 m, where the weight of the liners is transferred to the outer cylinder. Properties of the material of the chimney outer cylinder and liners are shown in **Table 1**. The peak displacement at the top of the RC cylinder under excitations is limited to 1/150 of its height according to the Chinese code GB 50135-2019 [25], and the limit value, in this case, is $u_{top,\lim}$ = H/150 = 1.44 m.
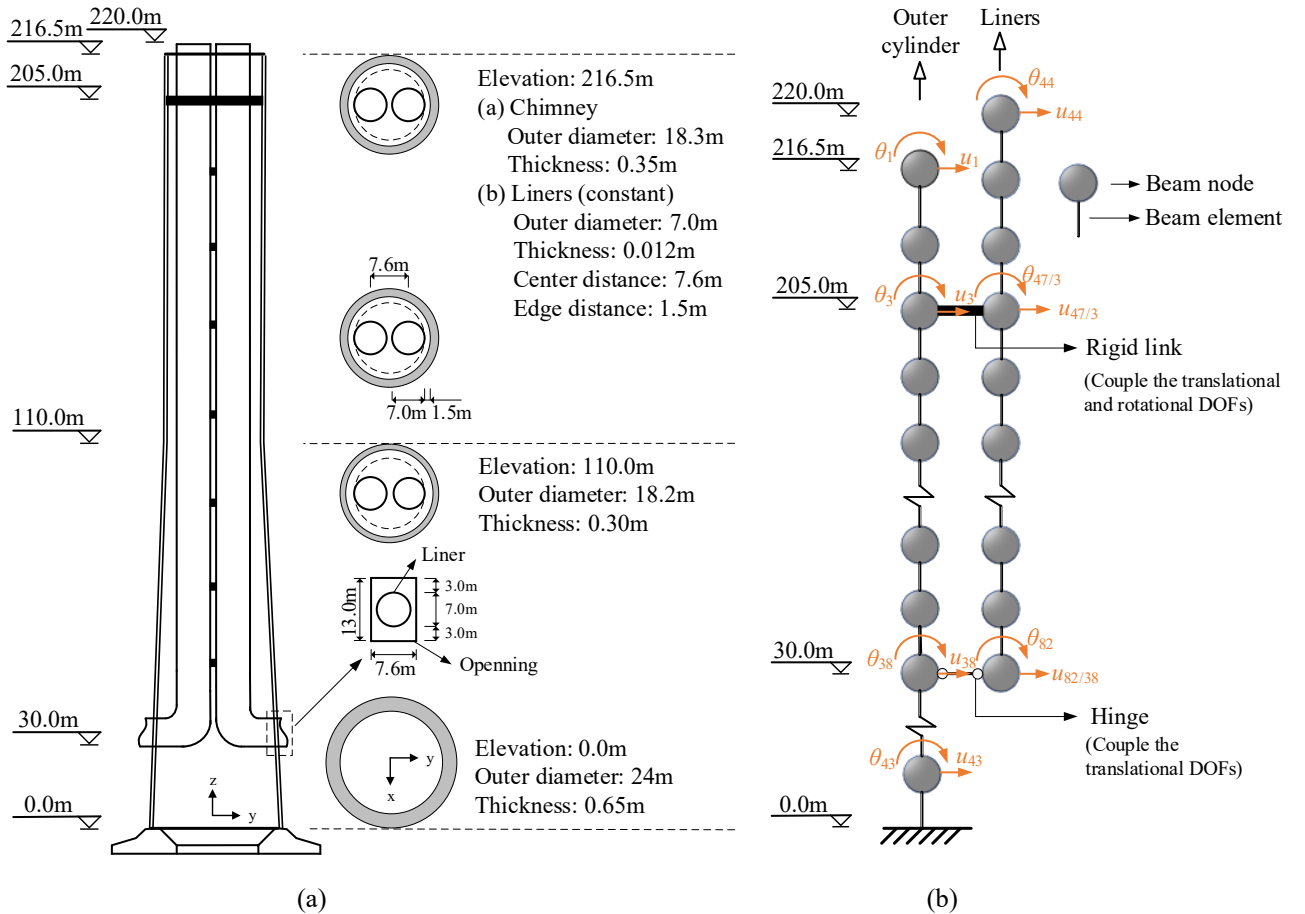

Fig. 1. (a) Schematic diagram of the chimney; (b) simplified model of original uncontrolled chimney.

Table 1. Properties of the material of the chimney outer cylinder and liners.

Structure section	Material	Young's modulus E (GPa)	Density ρ (kg/m³)	Poisson's ratio v
Outer cylinder	RC	28	2551	0.2
Liners	Steel	206	8010	0.3

2.2 Numerical modeling

A simplified planar 2D coupled model is proposed to conduct the numerical analysis of the uncontrolled chimney with liners. According to the simplified model, the outer cylinder and the liners are regarded as two independent beams and then coupled as shown in **Fig. 1**-(b). The detailed modeling process is as follows:

1) Discretize the outer cylinder and the liners in different sets of nodes and interconnecting elements. One translational and one rotational degree of freedom (DOF) are active in each node.

2) Establish the mass matrices of the outer cylinder and the liners expressed as $\mathbf{M_O}$ and $\mathbf{M_I}$, respectively, and the stiffness matrices expressed as $\mathbf{K_O}$ and $\mathbf{K_I}$, respectively, by means of Timoshenko beam theory. Apply the boundary conditions of the structure; the foundation is considered to be fully fixed in this study, representing the foundation on rock without losing generality in the results.

3) Conduct modal analysis of the outer cylinder individually and obtain its first two modal frequencies (ω_1 and ω_2) to establish the damping matrix of the RC outer cylinder $\mathbf{C_O}$ with the classical Rayleigh damping theory, as shown in Eq. (1). A damping ratio ξ of 0.01 is considered for the first two mode frequencies of the concrete cylinder [26]. The damping of the liners is ignored due to their low value and on the safe side.

$$\mathbf{C_O} = \frac{2\xi(\omega_1\omega_2)}{\omega_1 + \omega_2}\mathbf{M_O} + \frac{2\xi}{\omega_1 + \omega_2}\mathbf{K_O} \tag{1}$$

4) Combine the mass, stiffness and damping matrices of the outer cylinder and the liners directly to obtain the uncoupled matrices of the chimney-liners system: $\mathbf{M_L}$, $\mathbf{K_L}$ and $\mathbf{C_L}$, respectively, as:

$$\mathbf{M}_{\mathrm{L}} = \begin{bmatrix} \mathbf{M}_{\mathrm{O}} & \mathbf{0} \\ \mathbf{0} & \mathbf{M}_{\mathrm{I}} \end{bmatrix}; \quad \mathbf{K}_{\mathrm{L}} = \begin{bmatrix} \mathbf{K}_{\mathrm{O}} & \mathbf{0} \\ \mathbf{0} & \mathbf{K}_{\mathrm{I}} \end{bmatrix}; \quad \mathbf{C}_{\mathrm{L}} = \begin{bmatrix} \mathbf{C}_{\mathrm{O}} & \mathbf{0} \\ \mathbf{0} & \mathbf{0} \end{bmatrix} \tag{2}$$

5) Couple the degrees of freedom of the outer cylinder and the liners that are related by the connections between them and obtain the coupled matrices $\mathbf{M}$, $\mathbf{K}$ and $\mathbf{C}$. If we introduce a vector with all the translational (u) and rotational (θ) DOFs of the uncoupled system as $\mathbf{u} = (\mathbf{u}_{\mathrm{O}}, \mathbf{u}_{\mathrm{I}})^{\mathrm{T}}$, we can define a matrix $\mathbf{P}$ that relates the vector $\mathbf{u}$ with the DOFs of the structure included in $\mathbf{v}$, with $\mathbf{u} = \mathbf{P}\mathbf{v}$, in which $\mathbf{u}_{\mathrm{O}} = (u_1, \theta_1 \cdots u_m, \theta_m)$ is the DOFs of the outer cylinder; $\mathbf{u}_{\mathrm{I}} = (u_{m+1}, \theta_{m+1} \cdots u_{m+n+1}, \theta_{m+n+1})$ is the DOFs of the liners; m = 43 is the elements of the outer cylinder and n = 38 is the elements of the liners. The coupled mass, stiffness and damping matrices of the structure are expressed as:

$$\mathbf{M} = \mathbf{P}^{\mathrm{T}}\mathbf{M}_{\mathrm{L}}\mathbf{P}; \quad \mathbf{K} = \mathbf{P}^{\mathrm{T}}\mathbf{K}_{\mathrm{L}}\mathbf{P}; \quad \mathbf{C} = \mathbf{P}^{\mathrm{T}}\mathbf{C}_{\mathrm{L}}\mathbf{P} \tag{3}$$

Thus, the coupled equation of motion of the uncontrolled structure is:

$$\mathbf{M}\ddot{\mathbf{v}} + \mathbf{C}\dot{\mathbf{v}} + \mathbf{K}\mathbf{v} = \mathbf{F}_f \tag{4}$$

where $\mathbf{F}_f$ contains the external turbulent wind loads of the chimney. In addition, the static response of the structure under mean-wind loads can be obtained by solving the following equation:

$$\mathbf{K}\mathbf{v}_s = \mathbf{F}_s \tag{5}$$

where $\mathbf{F}_s$ is the vector with the mean wind actions on the chimney.

The assumptions of the proposed modeling strategy are as follows: a) the diameter and thickness are regarded to be constant for each element; b) the coupled structure is in the linear elastic state during the dynamic analysis; c) external loads are equivalent to the concentrated force acting on the beam nodes; d) the response of the structure is contained in the plane of the loads; and e) the liners are tied together by rigid constraints at several specific locations to make their relative motion negligible so that they respond to dynamic actions as a single unit. This is demonstrated in the next section by observing that

the lateral movements of the two liners of a shell-like model are almost identical in the low-order vibration modal shapes, as shown in **Fig. 3**. Furthermore, the supporting platform is considered to be rigid to couple the translational and the rotational DOFs of the outer cylinder and the liners at the elevation of 205 m, and the opening area is considered to be a hinge to couple their translational DOFs at the elevation of 30 m. Indeed, the flexibility of the supporting platform has an influence on the simulation result, and analysis conducted by the authors suggests that the top displacement response is significantly reduced with the rotational stiffness of the platform increasing from a relatively low value for most of the wind records tested.

2.3 Model validation

The flexural modes obtained with the simplified model are compared with the numerical solution provided by the commercial FE analysis software ABAQUS [27] using 4-node shell elements with reduced integration (S4R) in the regular domain, and introducing 3-node triangular shell (S3) elements locally to define the mesh close to the openings. After conducting a mesh-sensitivity study, a total of 2269 S4R elements and 17 S3 elements are used in the outer cylinder, and the liners are discretized with 1064 S4R elements. The base of the FE model is fully fixed. In addition, rigid multi-point constraints (MPC-beam in ABAQUS) are defined to integrate the two liners at 14 specific positions along their height, as shown in **Fig. 2**. The liners and the out er cylinder are linked by these rigid connections at the elevation of 205 m to enforce the constraints provided by the rigid supporting platform, and by constraints that couple the translational DOFs only in the opening area at the bottom part of the chimney. The first four flexural vibration mode frequencies in the y-z and x-z planes are compared in **Table 2** for the simplified and the FE models, and the corresponding modal shapes are included in **Fig. 3** (with a

magnitude factor of 22 units to facilitate visualization). It is observed that the modal shapes and the frequencies of the two models are very close, with a larger difference of 1.74 % in the y-z plane and a larger deviation of 4.80% in the x-z plane. This corresponds to the third mode and it is due to the warping deformation in the opening area of the concrete cylinder that cannot be captured in the simplified model, as highlighted in **Fig. 3**-(b). The modal analysis suggests the validity of the proposed simplified model, which will be used in the following to analyze the along-wind response.
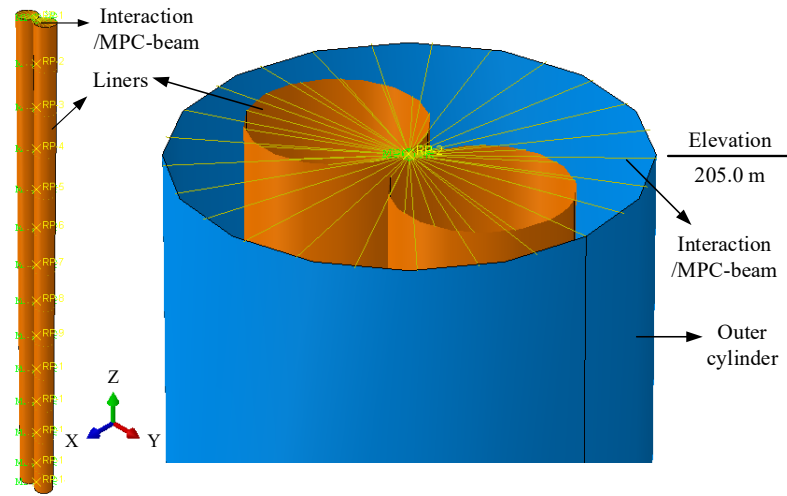

Fig. 2. Lateral links of the two liners and between the outer cylinder and the liners.

Table 2. Comparison of flexural mode frequencies between ABAQUS FE and simplified models in the y/x-z plane.

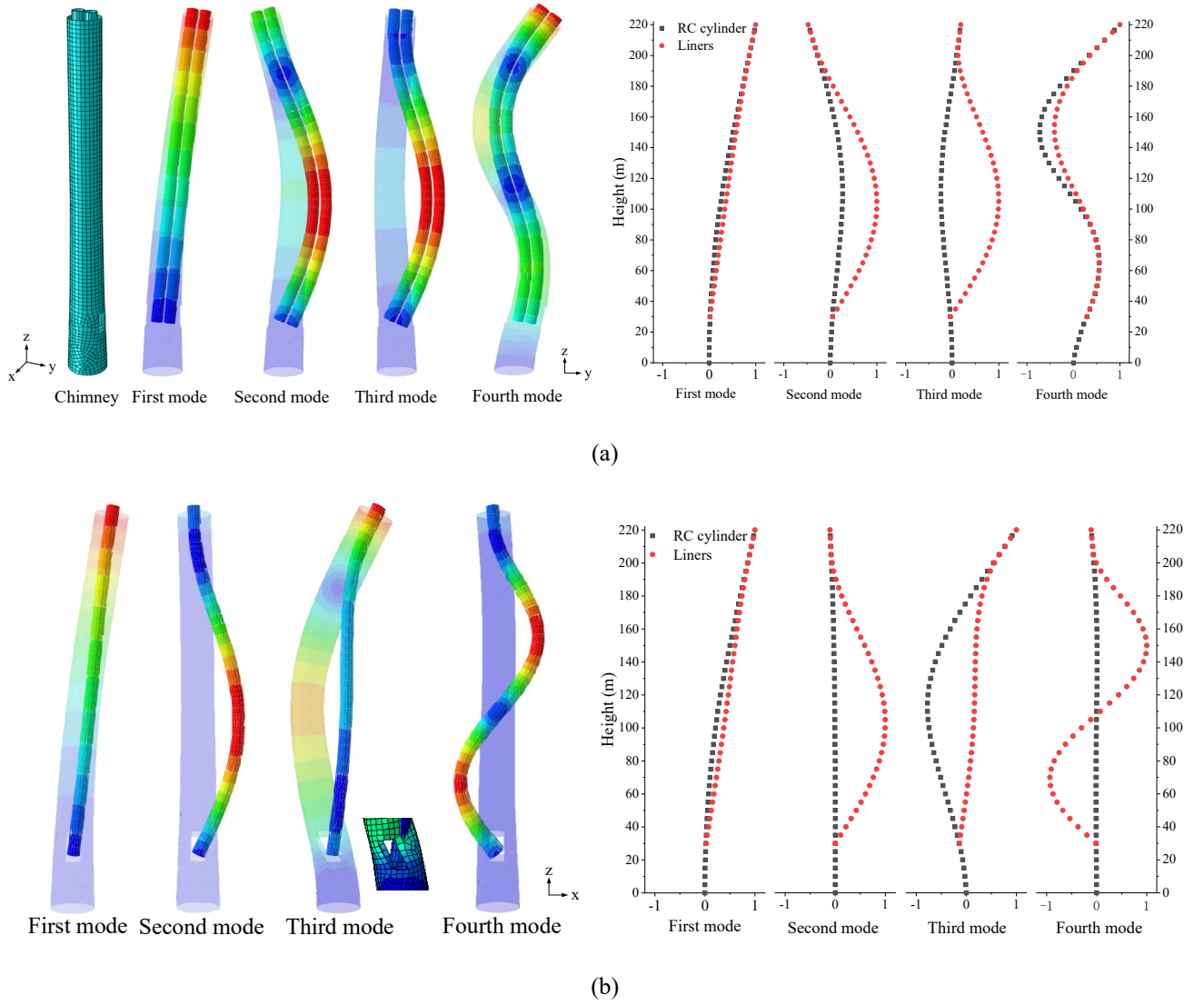| Plane	Model	First-mode frequency (Hz)	Second-mode frequency (Hz)	Third-mode frequency (Hz)	Fourth-mode frequency (Hz)
y-z	ABAQUS FE model	0.3459	1.6024	1.7693	3.9565
	Simplified model	0.3504	1.5901	1.7391	3.9333
	Deviation	1.28%	0.77%	1.74%	0.59%
x-z	ABAQUS FE model	0.3663	0.9817	1.5873	3.0968
	Simplified model	0.3656	0.9828	1.6674	3.0327
	Deviation	0.19%	0.11%	4.80%	2.11%

Fig. 3. Comparison of modal shapes of the chimney with liners between ABAQUS FE and simplified models in the (a) y-z plane and (b) x-z plane.

3 Along-wind response of the uncontrolled chimney

3.1 Along-wind load simulation

This work focuses on the along-wind response of the chimney and it ignores the across-wind movements induced by vortex shedding. The Consistent Discrete Random Flow Generation (CDRFG) technique is used to simulate the fluctuating wind loads according to the proposal of Aboshosha *et al.* [28], which generates turbulent wind-speed time histories based on the synthesizing random divergent-free turbulent

velocities. The resulting turbulent records have a better correlation for different frequencies compared with other methods of generating flows for large eddy simulation (LES). In addition, LES employing CDRFG produces structure responses that are in a very good agreement with those obtained from the boundary layer wind tunnel, and their spectra is very close to the target, in our case the Von Karman spectrum:

$$S_u(z,f) = \frac{4(I_u U)^2 (L_u/U)}{\left(1 + 70.8(f L_u/U)^2\right)^{5/6}} \tag{6}$$

where z (m) and f (Hz) are the height at the point in which the wind is simulated and the frequency, respectively. U is the mean along-flow wind speed defined as $U(z) = U_{ref}\left(z/z_{ref}\right)^{\alpha_U}$, and the subscript u refers to the along-flow properties. I_u is the turbulent intensity, $I_u(z) = I_{u,ref}\left(z/z_{ref}\right)^{-\alpha_I}$. L_u is the length scale of turbulence, $L_u(z) = L_{u,ref}\left(z/z_{ref}\right)^{\alpha_L}$. The classification of the wind site of the chimney is class D, with a reference height of z_{ref} = 10 m and a design wind speed at the reference height of U_{ref} = 57 m/s. According to the code ASCE 7-16 [29], the variation coefficient of wind speed with the height is α_U = 1/9 and the turbulence intensity at the reference height is $I_{z,ref}$ = 0.15, with α_I = 1/6. The turbulence integral length at the reference height is $L_{u,ref}$ = 198.12 m, with α_L = 1/8.

The CDRFG approach is used to generate a series of four independent time-history records of fluctuating wind speeds over a time of 10 min (600 s) with a frequency range between (0.01,10) Hz, a step of 0.2039 Hz, and a time-step of 0.01 second. The time-history records of the wind speed and the power spectrum density at the height corresponding to the top of the chimney are shown in **Fig. 4**, showing a good correlation for a wide range of frequencies containing those of the main structural modes.
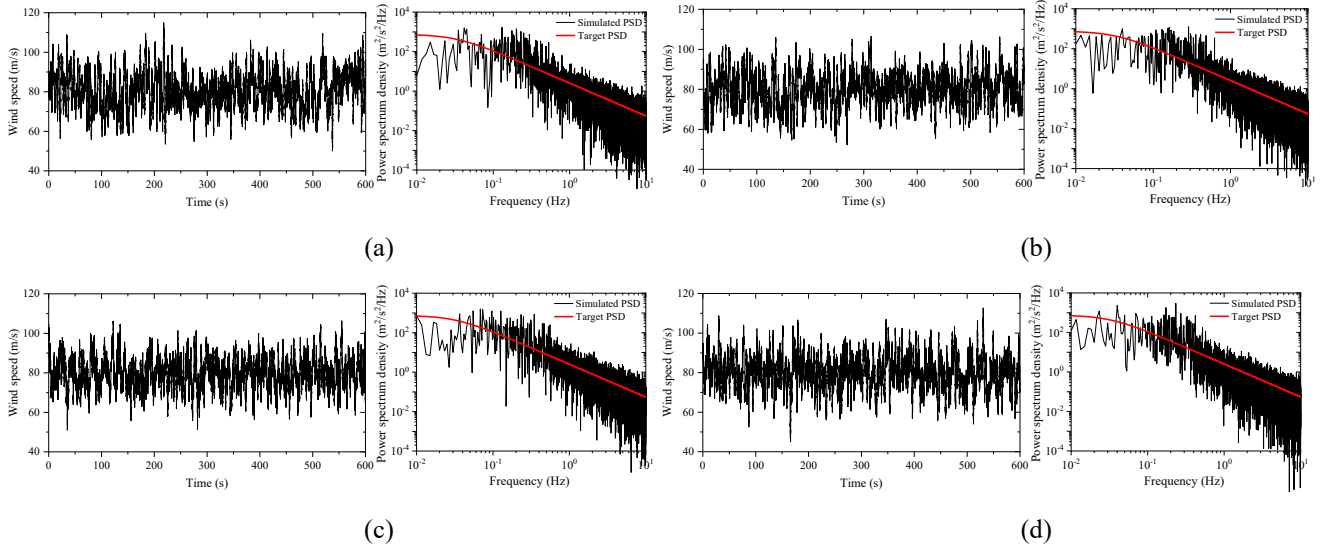
Fig. 4. A series of four independent time history records and their power spectrum density curves of wind speed at the top of the chimney. (a) Wind-1; (b) Wind-2; (c) Wind-3; (d) Wind-4.

According to the Davenport's quasi-steady assumption, the concentrated translational turbulent wind forces acting on the nodes of the simplified model can be obtained by:

$$F_f(i,t) = \rho V D L C_D u(i,t) \tag{7}$$

with their power spectrum densities defined as:

$$S_f(i,f) = \left(\rho V D L C_D\right)^2 S_u(i,f) \tag{8}$$

and the mean-wind forces of the nodes:

$$F_s(i,t) = \frac{1}{2}\rho V^2 D L C_D \tag{9}$$

where i represents the number of the node; D is the outer diameter of the element; L is the length of the element; V is the average wind speed at the height of the node; C_D is the aerodynamic drag coefficient, considered as 1.0 [6]; $\rho = 1.25$ kg/m^3 is the air density.

3.2 Structural analysis

The simplified numerical model of the uncontrolled chimney (as shown in **Fig. 1**-(b)) is implemented in MATLAB [30] using 161 DOFs. The Newmark-β's step-by-step iteration method is used to integrate the dynamic response of the chimney. Then, the dynamic response under turbulent wind forces obtained

from Eq. (7) is superimposed to the static response under mean-wind forces obtained from Eq. (9) to acquire the total response of the chimney.

The time histories of the top displacement and acceleration of the outer cylinder in the y-z plane (which is the plane selected to conduct all the analysis) are shown in **Fig. 5**. The static displacement at the top of the outer cylinder is 0.43 m and the amplitudes of the total displacement under the four wind histories are 1.57 m, 1.87 m, 1.48 m and 2.19 m, which exceed the limit value of 1.44 m.
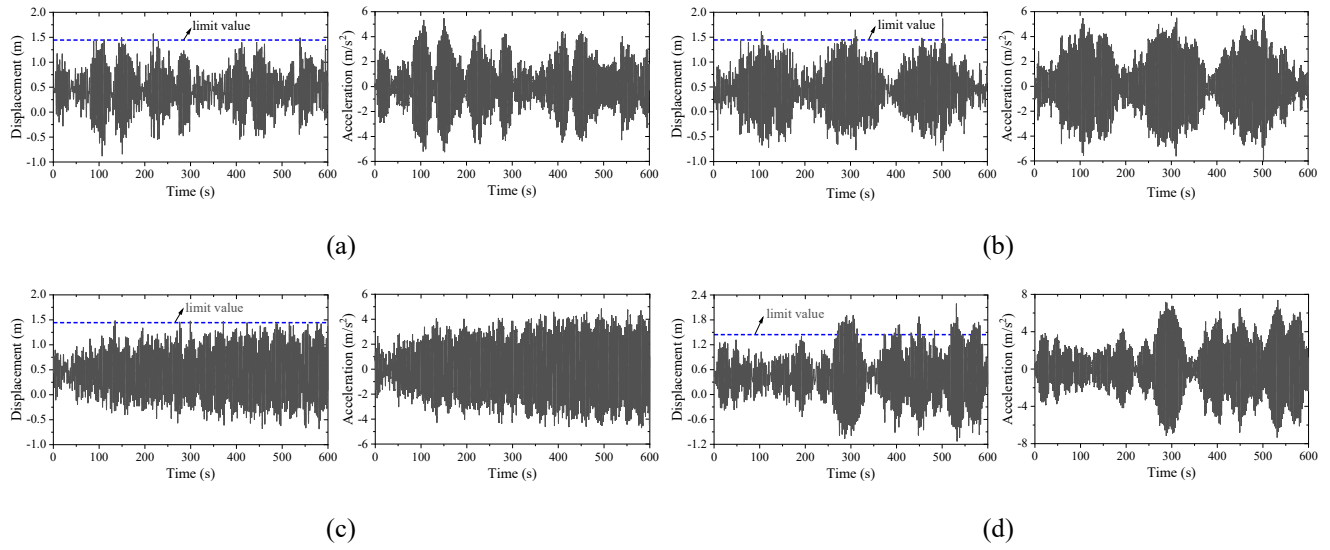

(a)

(b)

(c)

(d)

Fig. 5. Displacement and acceleration response of the top of the outer cylinder in the y-z plane under the actions of (a) Wind-1; (b) Wind-2; (c) Wind-3; (d) Wind-4.

4. Tuned-liners method and parameter optimization

4.1 Conceptual design

The liners of conventional chimneys are suspended by a rigid supporting platform that prevents relative movements between this element and the outer cylinder. This paper proposes to use the liners as a tuned mass to control the response of the outer cylinder, and separates them appropriately to allow their relative movements. The conventional supporting platform is replaced by horizontal tuning systems and vertical suspension systems, to promote the beneficial vibration of the liners relative to the concrete wall, as

shown in **Fig. 6**-(a). The suspension systems that are used to suspend the liners and transfer their gravity to the outer cylinder can provide large vertical stiffness to avoid significant vertical motion of the liners with negligible translational stiffness. The tuning systems can be designed with spring, damper, inerter and other mechanical elements. In this paper, a simple yet efficient tuning system that consists of a spring and a damper arranged in parallel is adopted. A total of eight of these tuning elements are uniformly distributed between the liners and the concrete cylinder in the radial direction, at the position where the original supporting platform was installed. The equivalent stiffness and damping coefficient of these tuning systems in the y-z plane are expressed as k_e and c_e, respectively. The corresponding simplified numerical model of the tuned structure for the dynamic analysis is shown in **Fig. 6**-(b).

The advantage of the proposed tuned liners is that it avoids adding large extra weight to control the structural vibration of chimneys, as it is the case in TMD and TLD solutions. The proposed method requires that there is sufficient space for the relative vibration of the outer cylinder and the liners whilst meeting the vibration limits of both systems. This is achieved by the selection of adequate parameters of the tuning systems as is explained in the following. The limit of the peak relative displacement of the outer cylinder and the liners at the height where the tuning systems are installed is considered as 1.0 m (the total space is 1.5 m) to guarantee the normal operation of the tuning system and the safety of the coupled structure. Thus, the performance requirements for the mitigation effect and the relative vibration control of the proposed method are introduced by considering the limit of the top and the relative displacements, respectively, as:

$$u_{top,\max} \leq u_{top,\lim} \tag{10}$$

$$u_{RD,\max} \leq u_{RD,\lim} \tag{11}$$

where $u_{top,\max}$ and $u_{top,\lim}$ are the recorded amplitude of the top displacement of the outer cylinder and its

corresponding limit, respectively; $u_{RD,\text{max}}$ and $u_{RD,\text{lim}}$ are the recorded amplitude of the relative

displacement of the outer cylinder and the liners at the elevation of 205 m where the tuning systems are

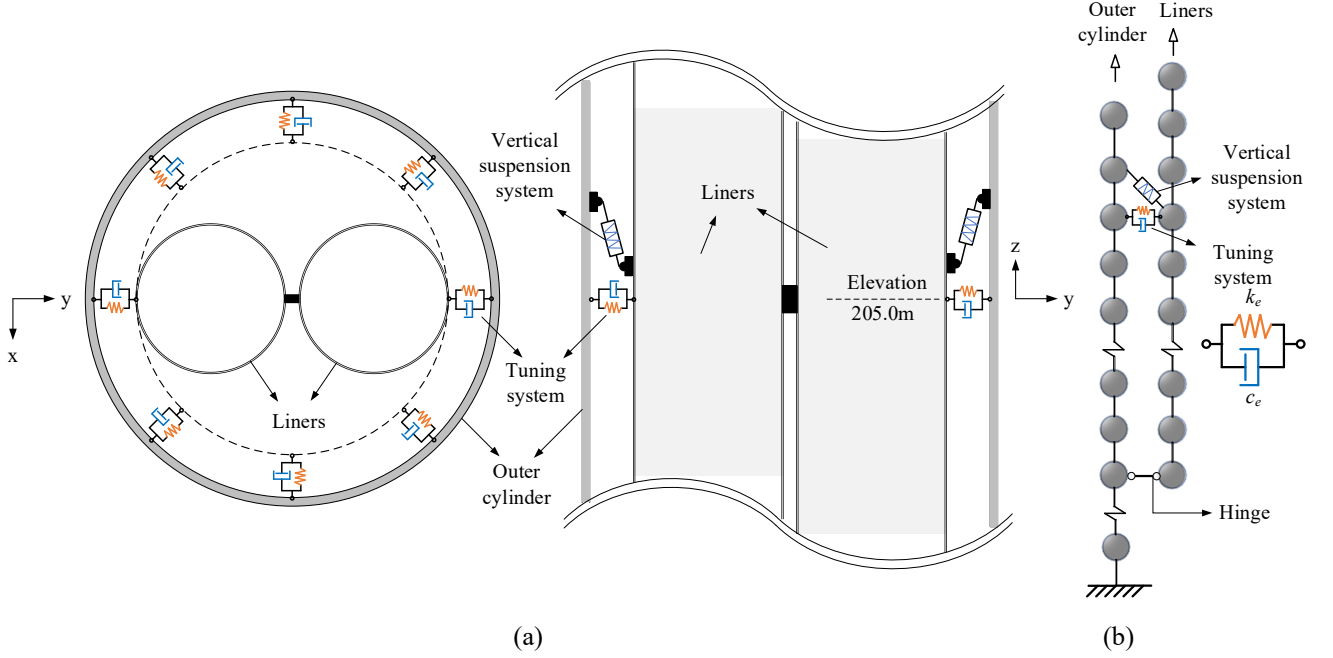installed and its corresponding limit, respectively.

(a)   (b)

Fig. 6. Proposed method of tuned liners. (a) Conceptual diagram; (b) numerical model of tuned structure.

4.2 Optimization strategy

For the application of the tuned-liners method, it is essential to obtain significant dynamic mitigation

effects with limited relative vibration of the outer cylinder and the liners. In terms of the dynamic

mitigation, the displacement and acceleration mitigation ratios of the top of the outer cylinder under

wind actions are introduced to evaluate the performance of the tuning systems in the time domain as:

$$\eta_{top} = 1 - \frac{u_{t,\text{rms}}^{top}}{u_{u,\text{rms}}^{top}}; \quad \gamma_{top} = 1 - \frac{a_{t,\text{rms}}^{top}}{a_{u,\text{rms}}^{top}} \tag{12}$$

where η_{top} and γ_{top} are the displacement and the acceleration mitigation ratio, respectively; $u_{u,\text{rms}}^{top}$ and $a_{u,\text{rms}}^{top}$

are the root-mean-square (RMS) values of the displacement and the acceleration of the top of the

uncontrolled chimney, respectively; $u_{t,\text{rms}}^{top}$ and $a_{t,\text{rms}}^{top}$ are the RMS of the displacement and the acceleration

of the top of the tuned chimney, respectively.

To obtain the optimal parameters of the tuning system in the simplified model considering the performance of the mitigation effect in the frequency domain, the second norm theory based on the top displacement is adopted to select the parameters for the pre-optimization. The second norm of the displacement of the structure is expressed as:

$$\sigma = \sqrt{\int_{-\infty}^{+\infty} |\mathbf{H}(i\omega)|^2 \mathbf{S}_f(\omega) d\omega} \tag{13}$$

where $\mathbf{S}_f(\omega)$ is the target power spectrum densities of wind forces obtained by Eq. (8); $\mathbf{H}(i\omega)$ is the transfer function of the structure expressed as:

$$\mathbf{H}(i\omega) = \left(-\omega^2 \mathbf{M} + i\omega \mathbf{C} + \mathbf{K}\right)^{-1} \tag{14}$$

Thus, the mitigation ratio of the root-mean-square value is defined as:

$$\beta_{top} = 1 - \frac{\sigma_t^{top}}{\sigma_u^{top}} \tag{15}$$

where σ_u^{top} and σ_t^{top} are the second norm of the top displacement obtained by Eq. (13) of the uncontrolled and controlled structures, respectively.

In addition, according to the tuning system described above, the parameters of the tuning system in the simplified model are defined by their dimensionless forms as:

$$f_t = \frac{\omega_t}{\omega_u}; \quad \xi_t = \frac{c_e}{2m_I \omega_t} \tag{16}$$

in which $\omega_t = \sqrt{k_e / m_I}$; ω_u is the first circular frequency of the outer cylinder; m_I is the total mass of the liners; k_e and c_e are the equivalent stiffness and damping coefficient of the tuning system in the simplified model. Thus, the pre-optimization that is conducted to obtain a significant controlling effect of the top displacement and optimized parameters $f_{t,opt}$ and $\xi_{t,opt}$ of the tuning system can be formulated as:

$$\text{maximize} \qquad \beta_{top}$$
$$\text{subjected to} \quad \begin{cases} f_{t,\min} \le f_t \le f_{t,\max} \\ \xi_{t,\min} \le \xi_t \le \xi_{t,\max} \end{cases} \qquad (17)$$

However, the tuning system designed by Eq. (17) may have a good controlling effect of displacement but may not meet the performance requirement in terms of the relative response $u_{RD,\max}$. To consider the relative vibration constraint of the outer cylinder and the liners that is not considered in the pre-optimization process, time-history analysis for the four wind velocity records is conducted to obtain the peak relative displacements $u_{RD,\max}$. In this study the performance in terms of the relative response is obtained by comparing the peak value with the limit value in the dynamic analysis. The parameters of the tuning system obtained by solving Eq. (17) are adjusted to meet this performance requirements providing the $u_{RD,\max}$ exceeds the limit value. In this study, the damping coefficient $\xi_{t,opt}$ is increased gradually with a fixed $f_{t,opt}$ obtained by Eq. (17) until the value of $u_{RD,\max}$ is smaller than the limit value, and the adjusted damping coefficient is defined as:

$$\lambda = \frac{\xi'_{t,opt}}{\xi_{t,opt}} \qquad (18)$$

where $\xi'_{t,opt}$ is the dimensionless adjusted damping coefficient, and λ is the increasement ratio of $\xi_{t,opt}$. Thus, a design process for the tuned-liners method under along-wind actions considering the controlling effect and relative vibration limit is presented in **Fig. 7**.
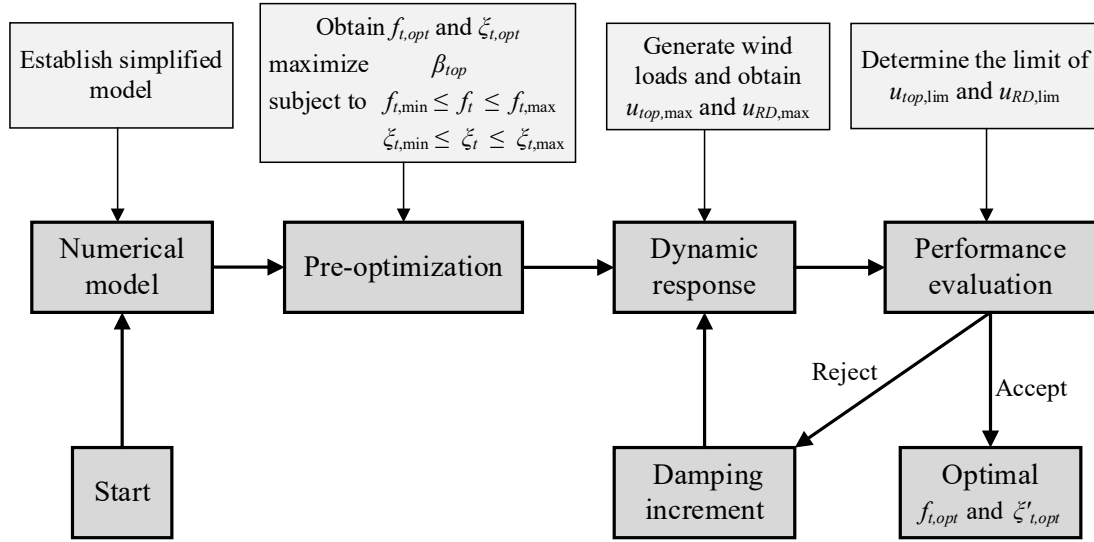
Fig. 7. Design flow chart proposed for chimneys with tuned liners.

4.3 Case study

According to the proposed design process discussed, the parameter optimization for the tuning system and the performance evaluation of the chimney described in Section 2 in the y-z plane are conducted as follows: ~~In a separate study not presented here due to space constraints, we have applied the wind loading in the x-z and y-z planes independently, to observe that the response is very similar and the proposed control technique is efficient regardless of the wind direction. In the following, only the optimization process and response in the y-z plane are included.~~

1) *Numerical model.* The tuned chimney is implemented using the simplified model that is analogous to that described for the uncontrolled chimney.

2) *Pre-optimization.* The second norm and the corresponding mitigation ratio of the top displacement of the tuned structure are calculated with the value of ω in the interval 2π (0.01,10) rad, and the parameters f_t and ξ_t range from 0.50 to 0.65 and 0.08 to 0.14, respectively. **Fig. 8** shows the results in the proposed chimney, which gives the following pre-optimum parameters $f_{t,opt} = 0.578$ and $\xi_{t,opt} = 0.108$.
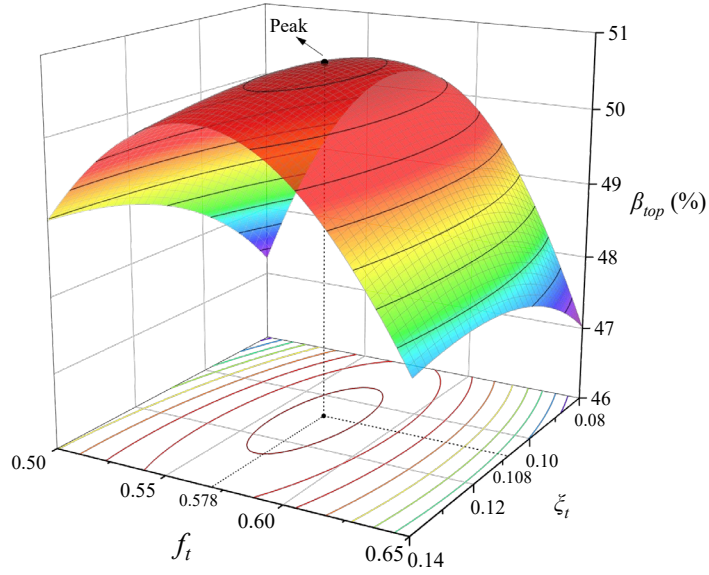
Fig. 8. Parameters influence of f_t and ξ_t to β_{top}.

where $\beta_{top} = 1 - \sigma_t^{top}/\sigma_u^{top}$ is the mitigation ratio of the root-mean-square value of the top displacement

defined in Eq. (15).

3) *Dynamic response.* The wind loads are applied to the uncontrolled chimney and also to the controlled

chimney with pre-optimum tuning parameters obtained previously. In the proposed chimney, the

results of the dynamic time-history analysis show that the amplitudes of the top displacements of the

outer cylinder are 1.14 m, 1.02 m, 0.87 m and 1.01 m, respectively, and the peak relative

displacements of the outer cylinder and the liners at the height where the tuning system is located are

1.09 m, 0.95 m, 0.83 m and 1.12 m, respectively.

4) *Performance evaluation.* The performance of the tuned structure is evaluated from the mitigation

ratio η_{top} and the peak relative displacement $u_{RD,\max}$. In the proposed structure it is observed that the

tuning system has a good performance for the top displacement control because the amplitudes of the

top displacements of the tuned structure are significantly smaller than the limit value of 1.44 m, which

will be discussed in more detail later. However, the relative displacements under two of the wind

histories (Records 1 and 4) exceed the 1-m limit at the height where the tuning system is located.

Thus, the parameter related to damping coefficient $\xi_{t,opt}$ introduced above has to be adjusted to meet this performance requirement.

5) *Damping increment*. The damping coefficient of the tuning system is increased to reduce the relative displacement of the outer cylinder and the liners. **Fig. 9** shows the relationship between λ and $u_{RD,max}$ for the four wind histories. From the figure, λ is selected at the performance point where the maximum of the four $u_{RD,max}$ is equal to the limit value $u_{RD,lim}$. Thus, the relative responses under the four wind histories are all within the limit at this point. In this case, the parameter λ is selected as 1.26 to satisfy the performance requirement for the relative vibration, resulting in $\xi'_{t,opt} = 0.137$.
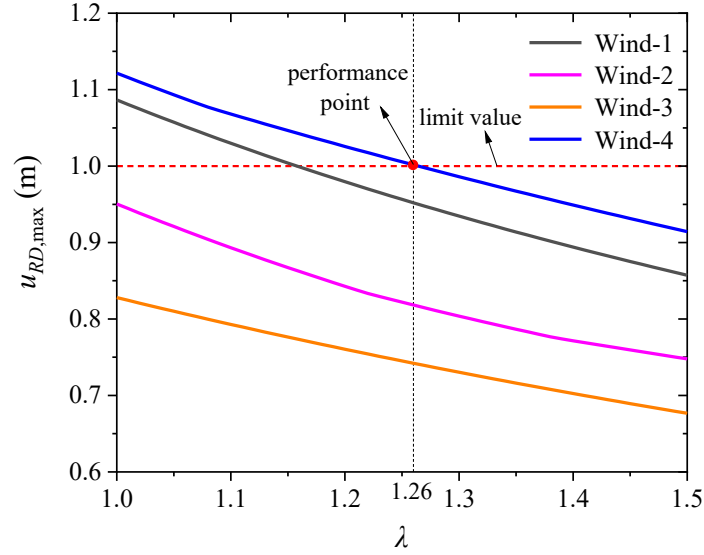

Fig. 9. Parameter influence of λ (= $\xi'_{t,opt} / \xi_{t,opt}$) to $u_{RD,max}$.

6) *Dynamic response recalculation and performance reevaluation*. The adjusted parameter $\xi'_{t,opt}$ is applied for the dynamic analysis of the tuned structure. In the proposed structure this leads to the amplitudes of the top displacement of the outer cylinder of 1.14 m, 1.05 m, 0.90 m, 1.04 m for the four wind records, and the amplitudes of the relative displacement are 0.95 m, 0.82 m, 0.74 m, 0.998 m. By comparing with the amplitudes of the relative displacement in Step 3), it can be observed that they are reduced and satisfy now the limitation. In addition, the performance requirement in terms of

the mitigation effect is still significantly satisfied.

The optimal parameters of $f_{t,opt}$ and $\xi'_{t,opt}$ resulted from this design method in the proposed chimney are 0.578 and 0.137, respectively. This corresponds to the stiffness and damping coefficient of the tuning system in the simplified model of k_e = 1419 kN/m and c_e = 292 kN·m/s, respectively.

In order to investigate the effectiveness of the damping-increment strategy described above on the performance design, a comprehensive parametric study is conducted. **Fig. 10** illustrates the impact of the parameters f_t and ξ_t on the mitigation ratio of the second norm of the top displacement from the pre-optimized result, indicating that the mitigation ratio of the second norm of top displacement β_{top} is relatively insensitive to the change of ξ_t or λ compared with that to the change of f_t.
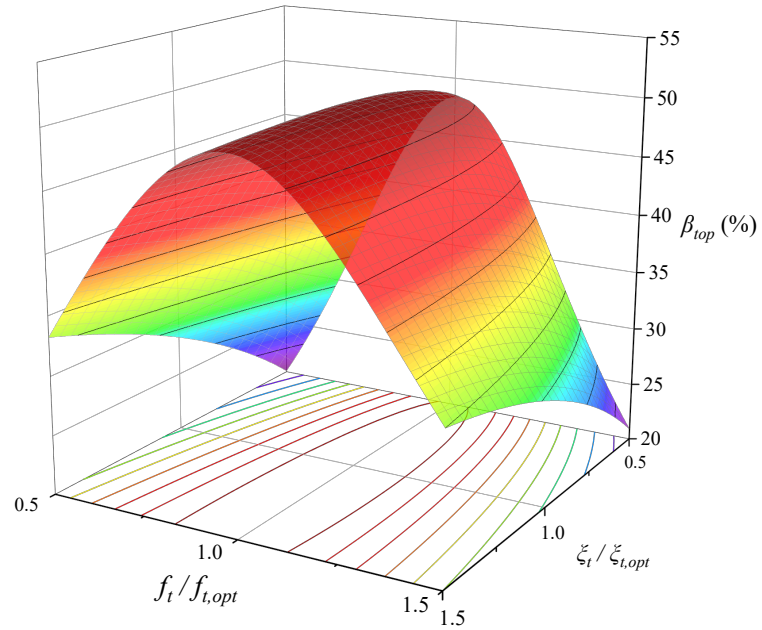

Fig. 10. Sensitivity analysis of f_t and ξ_t to β_{top}.

The influence of the parameter λ on the peak relative displacement, the mitigation effect of the top displacement and the acceleration under the four wind actions is further studied considering the parameter λ ranging from 0.5 to 2.0, and the parameter $f_{t,opt}$ is fixed. The results are shown in **Fig. 11** and it is observed that the mitigation ratios of the top displacement and acceleration are relatively insensitive

to the parameter λ. On the contrary, the peak relative displacement decreases rapidly with the increment of λ. This indicates that the relative vibration of the outer cylinder and the liners can be effectively reduced with small variation of the mitigation effect by increasing the damping coefficient of the tuning system. Thus, increasing the damping to satisfy the performance requirements is a reliable strategy for the performance design of the tuning properties.
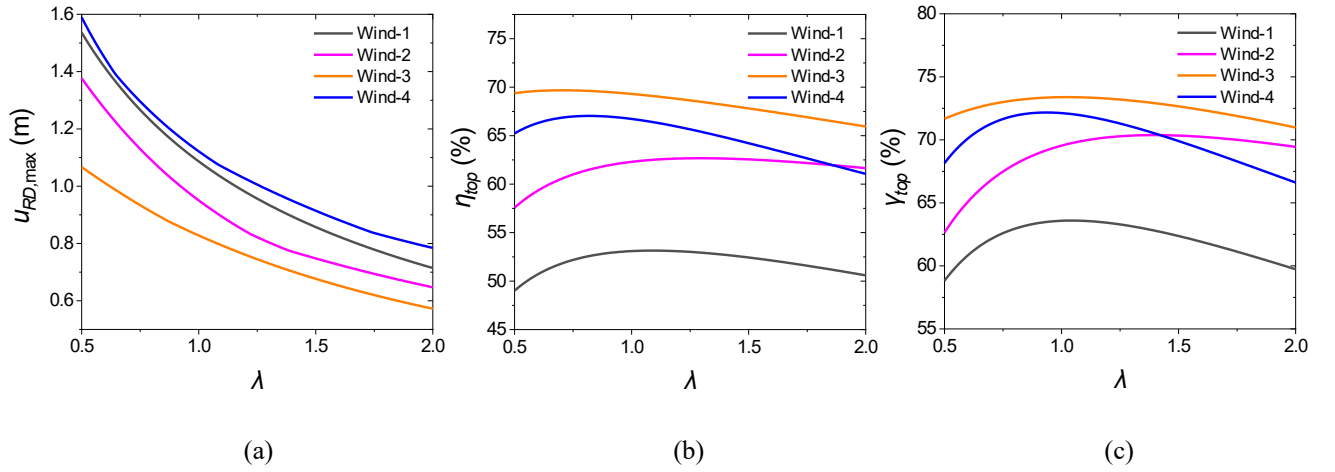

Fig. 11. The influence of parameter λ ($= \xi'_{t,opt} / \xi_{t,opt}$) on (a) the peak relative displacement, (b) the mitigation ratio of top displacement and (c) top acceleration under the actions of the four wind records.

5 Reduction effect analysis

In the following, analysis of the reduction performance in terms of the top displacement, top acceleration and the bending stress at the opening aera is conducted to demonstrate the effectiveness of the tuned chimney. In addition, the traditional TMD solution is compared with the proposed tuned chimney to show the advantages of the tuned liners, and the reduction performance in the perpendicular direction presented.

5.1 reduction performance of the tuned chimney

Time history analysis is conducted to observe the reduction effect of the proposed method with the

optimal parameters obtained in the previous section. The comparison between the response of the uncontrolled and the tuned chimney is based on the mitigation ratios defined as Eq. (12). It is noted that the numerical model of the uncontrolled and the tuned chimneys are illustrated in **Fig. 1**-(b) and **Fig. 6**-(b), respectively; the dynamic analysis of the uncontrolled chimney is implemented in Section 3.2. Thus, the time history curves of the top displacement and acceleration of the outer cylinder are shown in **Fig. 12**. The results show that the proposed tuned-liners method has a significant controlling effect on the along-wind displacement and acceleration response of the chimney with liners.

$u_{u,rms}^{top} = 0.40m \quad u_{t,rms}^{top} = 0.19m \quad \eta_{top} = 52.50\%$ $\quad$ $a_{u,rms}^{top} = 1.86\,m/s^2 \quad a_{t,rms}^{top} = 0.68\,m/s^2 \quad \gamma_{top} = 63.44\%$

(a)

$u_{u,rms}^{top} = 0.46m \quad u_{t,rms}^{top} = 0.17m \quad \eta_{top} = 63.04\%$ $\quad$ $a_{u,rms}^{top} = 2.17\,m/s^2 \quad a_{t,rms}^{top} = 0.64\,m/s^2 \quad \gamma_{top} = 70.51\%$

(b)

$u_{u,rms}^{top} = 0.48m \quad u_{t,rms}^{top} = 0.15m \quad \eta_{top} = 68.75\%$ $\quad$ $a_{u,rms}^{top} = 2.25\,m/s^2 \quad a_{t,rms}^{top} = 0.60\,m/s^2 \quad \gamma_{top} = 73.33\%$
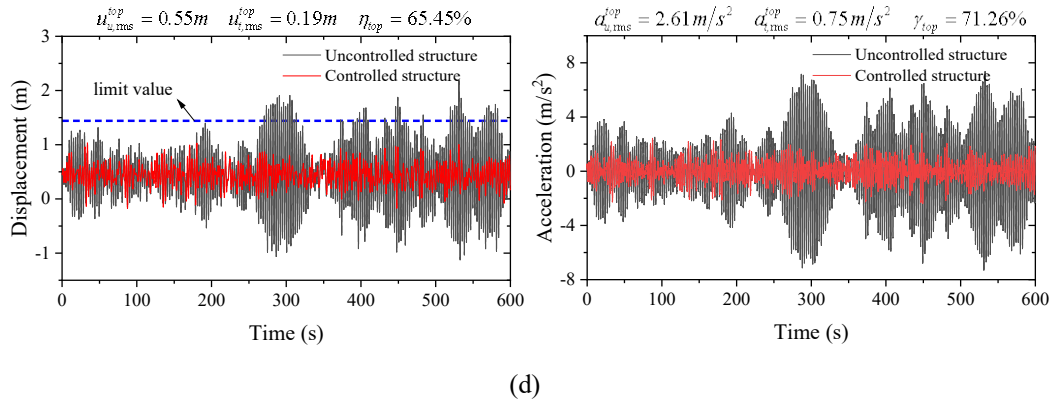
(c)

Fig. 12. Comparison of top displacement and top acceleration of the controlled and the uncontrolled chimneys under the actions of (a) Wind-1; (b) Wind-2; (c) Wind-3; (d) Wind-4. (η_{top} and γ_{top} are the mitigation ratios of the top displacement and acceleration, respectively, as defined in Eq. (12)).

Apart from the reduction effect of top displacement and acceleration, the bending stress at the opening area is also a key safety criterion that needs to be assessed. The bending stress at the elevation of 30 m, where the openings are located, can be obtained from the analysis of the beam-like numerical model, as:

$$\sigma_{max} = \frac{|M|_{max} \, y}{I} \tag{19}$$

where I is the moment of inertia of the cross-section under consideration; y is the perpendicular distance from the geometrical center of the cross-section to its edge; M is the bending moment at that position under turbulent wind and the mean-wind actions. The results of the peak bending stresses during the wind excitation are shown in **Table 3**. It is observed that the peak bending stress is reduced to a very low level with the tuned liners applied. However, this calculation of stresses cannot capture the stress concentration around the orifice, which would need to be addressed in further research works using detailed shell models.

Table 3. Amplitudes of bending stress of the uncontrolled and the controlled chimneys at the opening area under the action of the four wind records (MPa).

Structure	Wind-1	Wind-2	Wind-3	Wind-4
Uncontrolled	31.08	36.74	29.32	43.20

| Controlled | 22.57 | 20.62 | 18.06 | 20.34 |

5.2 Comparison with TMD

In order to further explore the advantage of the proposed method, a control strategy with conventional TMD is conducted to find out the additional mass needed in the TMD system to match the reduction effect of the tuned-liners structure. The mechanical model of a TMD and the corresponding controlled structure are shown in **Fig. 13**. The TMD system is located at the elevation of 205 m. The second norm of displacement of the chimney with TMD (σ_{TMD}^{top}) can be also obtained by Eq. (13), and the mitigation ratios of the root-mean-square value are defined in Eq. (15). The dimensionless parameters of the TMD system are defined as:

$$\mu_t = \frac{m_d}{m_T}; \quad \mu_k = \frac{\omega_d}{\omega_T}; \quad \mu_c = \frac{c_d}{2m_d\omega_d} \tag{20}$$

where m_d and c_d are the tuned mass and the damping of the TMD system, respectively; $\omega_d = \sqrt{k_d/m_d}$, and k_d is the stiffness of the TMD system; $\omega_T = 2.2016$ rad is the first circular frequency of the uncontrolled chimney. $m_T = 5.565 \times 10^6$ kg is the modal mass corresponding to the first mode, and it is calculated as $m_T = \sum |\varphi_i|^2 m_i$, in which φ is the shape corresponding to the first mode of vibration and $\|\varphi\| = 1$, and m_i is the mass of the i-th element of the structure.

The optimization function of the conventional TMD to achieve the same reduction effect as that of the proposed solution can be formulated as:

$$
\begin{aligned}
\text{minimize} \quad & (\mu_t) \\
\text{subject to} \quad & \begin{cases} \mu_{k,\min} \leq \mu_k \leq \mu_{k,\max} \\ \mu_{c,\min} \leq \mu_c \leq \mu_{c,\max} \\ \beta_{top}^{TMD} \geq \beta_{top}^{L} \end{cases}
\end{aligned} \tag{21}
$$

where $\beta_{top}^{TMD} \left(= \left\|1 - \sigma_{TMD}^{top}/\sigma_u^{top}\right\|\right)$ and $\beta_{top}^{L} (= 50.43\%)$ are the maximum mitigation ratios of the root-mean-square value of the structure with TMD and with the proposed method applied, respectively. **Fig. 14**

shows the relationship between μ_t and the corresponding maximum mitigation ratio β_{top}^{TMD}, indicating that

an additional mass of 2.99×10^5 kg (i.e., almost 300 tons, $\mu_t = 5.4\%$) would be required to obtain the same

reduction effect as that using the proposed method. Dynamic analysis of the structure under along-wind

actions with the optimal parameters corresponding to point E in this plot is conducted, and the

comparison of the mitigation ratios (the same definition as Eq. (12)) of the RMS value of the top

displacement and acceleration is shown in **Table 4.** Comparison of the reduction effect between the two

solutions under the four wind records. for different control solutions. It is observed that the reduction

effect of the controlled structures with TMD solution and the proposed solution is very close in the time

domain. Thus, the proposed method could effectively reduce the along-wind response and avoid having

to introduce a mass of approximately 300 tons near the top of the structure.
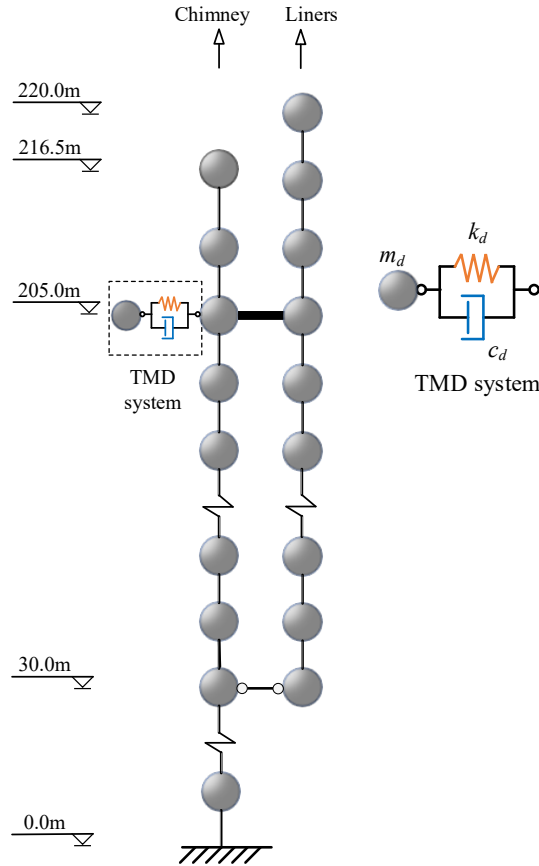

Fig. 13. Numerical model of the chimney with TMD and the mechanical model of a TMD.
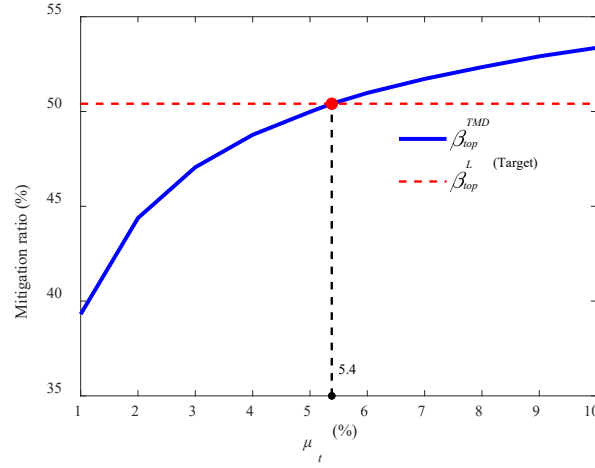
Fig. 14. Relationship between μ_t and $\beta_{top}^{TMD}\left(=\left\|1-\sigma_{TMD}^{top}/\sigma_u^{top}\right\|\right)$.

Table 4. Comparison of the reduction effect between the two solutions under the four wind records.

Solution	Mitigation ratio	Wind-1	Wind-2	Wind-3	Wind-4
TMD	Displacement	50.91%	61.31%	69.21%	65.72%
	Acceleration	62.98%	70.52%	75.72%	72.52%
Tuned liners	Displacement	52.50%	63.04%	68.75%	65.45%
	Acceleration	63.44%	70.51%	73.33%	71.26%

5.3 Reduction performance in the perpendicular direction

The previous analysis focused on the response in the y-z plane because it contains the lower orifice in which piping constrains the structure. However, the response in the perpendicular direction (or the x-z plane, as illustrated in **Fig. 1**-(a), **Fig. 2** and **Fig. 6**) is presented here to demonstrate the feasibility of the proposed chimney in multiple directions.

A new numerical model is developed to represent the coupled structural motion in the x-z plane using the simplified beam-like model as described in Section 2.2, and the effectiveness of the model has been demonstrated in Section 2.3 by comparing its first four flexural modes with the detailed shell model. The optimization is conducted in accordance with the method described in Section 4.3. **Table 5** shows the analysis results and the reduction effect in the x-z plane under the four wind actions that has been

used to analyze the response in the y-z plane. The results illustrate the significant reduction of the vibration under the wind records #1 and #4, which are the most critical ones, and that the performance in terms of the reduction effect in both the y-z plane and the x-z plane is significantly improved by the proposed method of tuning the liners in both principal directions.

Table 5. Reduction effect of the tuned structure in the x-z plane

Wind	$u_{u,\max}^{top}$ (m)	$u_{t,\max}^{top}$ (m)	$u_{u,\mathrm{rms}}^{top}$ (m)	$u_{t,\mathrm{rms}}^{top}$ (m)	$a_{u,\mathrm{rms}}^{top}$ (m/s^2)	$a_{t,\mathrm{rms}}^{top}$ (m/s^2)	$u_{RD,\max}$ (m)	η_{top}	γ_{top}
1	1.8400	1.0000	0.4768	0.1611	2.4368	0.6309	0.7518	66.22%	74.11%
2	1.1358	0.9215	0.2194	0.1503	1.0173	0.6145	0.6868	31.48%	39.60%
3	0.9184	0.8345	0.1945	0.1387	0.8866	0.6334	0.5880	28.79%	28.55%
4	1.8523	0.9227	0.4734	0.1671	2.4090	0.6974	0.8408	64.70%	71.05%

6 Safety performance analysis

This section assesses the safety of the chimney operation by assessing the relative vibration of its components, the specific restraints at the lateral openings and the effect unintentional eccentricities due to e.g. construction misalignments.

6.1 Relative vibration between the outer cylinder and the liners

The relative displacements of the outer cylinder and the liners in the y-z plane at the elevation of 205 m where the tuning system is located in the simplified model are presented in **Fig. 15** with the optimal parameters. They are below the 1.0-m limitation in the entire excitation.
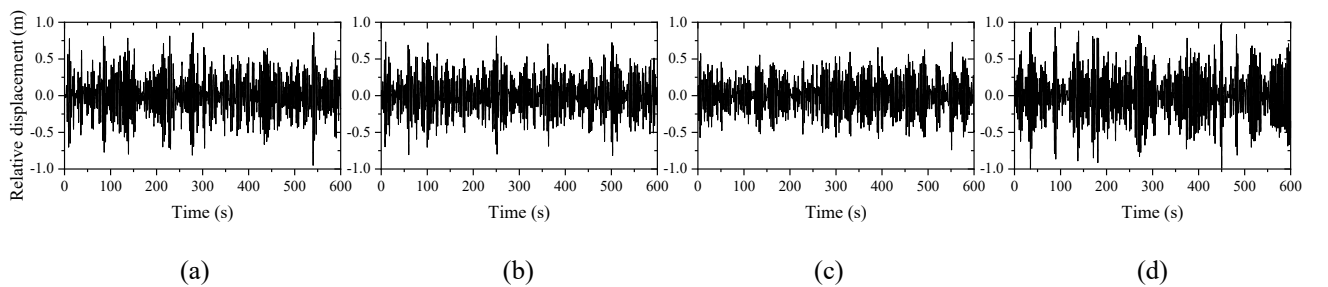

(a) (b) (c) (d)

The movements between the outer cylinder and the liners are further explored in **Fig. 16**, where the peak displacements and the peak relative displacements along the height of the structure under the four wind actions are presented for the uncontrolled and controlled cases. The results demonstrate that the vibration of the outer cylinder is greatly suppressed using the tuned liners at the expense of increasing the relative displacement of the outer cylinder and the liners. However, these values are within the admissible limit as mentioned previously. Indeed, the peak relative displacements between the RC cylinder and the liners appear at the top of concrete part, and they are 0.985 m, 0.849 m, 0.777 m and 1.040 m, respectively, under the four wind actions, which however are very close to the values on the elevation of 205 m. Moreover, we note that P-Delta effects are not considered in this work and preliminary analysis suggests that they may amplify the absolute and relative responses of the tuned scheme, which would need detailed analysis in future research.
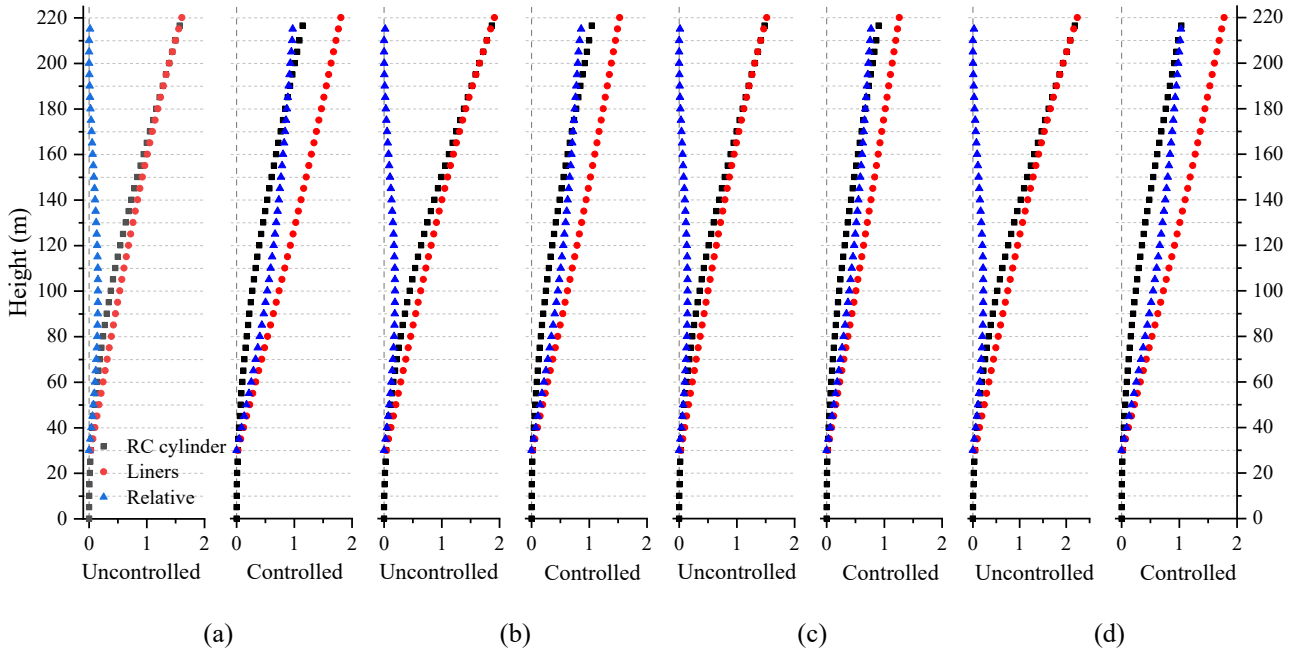

Fig. 16. Peak absolute/relative displacements (m) along the height of the uncontrolled and controlled structure under the actions of (a) Wind-1; (b) Wind-2; (c) Wind-3; (d) Wind-4.

6.2 Lateral openings restraint

Apart from checking the relative liner-concrete displacements, the movements of the liners at the orifices of the outer cylinder need to be checked, even if this is not considered as part of the design process because it is rarely a governing criterion. As shown in **Fig. 1**-(a), the liners are cut the outer cylinder at the height of 30 m. The link of the outer cylinder and the liners are considered as a hinge that avoids the translational relative displacement but allows the relative rotation at the height which potentially produces impacts between the horizontal part of the liner and the concrete wall in the y-z plane. At this position, the geometric center of the coupled liners is regarded as the rotation center, and the motion of the extended part of the liners as a rigid-body rotation. In addition, the distance between the rotation center and the inner wall of the opening is about 10.2 m, and the distance between the liner and the concrete wall is 3.0 m, thus the allowable rotation angle is: $\theta_{lim} = \arctan (3.0/10.2) = 0.2861$ rad.

The time histories of the relative rotation between the liner and the concrete around the x axis (i.e., in the y-z plane) at the level of the lateral orifices of the concrete are shown in **Fig. 17**. The results show that the peak relative angles are about 0.0093 rad, 0.0079 rad, 0.0066 rad and 0.0093 rad, respectively which are far smaller than the allowable value. This confirms that there is no risk between the liner and the concrete at the orifice.
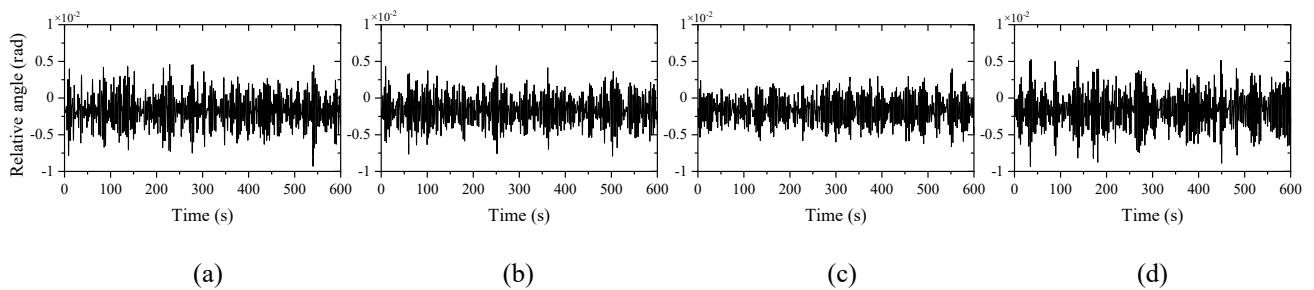

(a)   (b)   (c)   (d)

Fig. 17. Time histories of relative angle between the liner and the concrete wall at the lateral orifices under the actions of (a) Wind-1; (b) Wind-2; (c) Wind-3; (d) Wind-4.

6.3 Analysis of unintentional eccentricities

In the construction of the chimney or in the installation of the tuning systems, unintentional eccentricities may occur, for instance the out-of-plumb of the mass or small rotations of the chimney at its base. These effects are studied now using the simplified beam-like. We take separately the following two effects into consideration: 1) a small offset (Δ) of the liners at the place where the tuning systems are located due to the accidental eccentricities of the lining or assembly error, as shown in **Fig. 18**-(a), and 2) the addition of a small rotation (α) of the chimney at the base, as shown in **Fig. 18**-(b).

To account for the initial rotation of the beam-like model its coordinates are affected by the rotation matrix

$$
\begin{aligned}
u_i &= \bar{u}_i \cos(\alpha) - \bar{v}_i \sin(\alpha) \\
v_i &= \bar{u}_i \sin(\alpha) + \bar{v}_i \cos(\alpha) \\
\theta_i &= \bar{\theta}_i
\end{aligned}
\Rightarrow
\begin{Bmatrix} u_i \\ v_i \\ \theta_i \end{Bmatrix}
=
\begin{bmatrix} \cos(\alpha) & -\sin(\alpha) & 0 \\ \sin(\alpha) & \cos(\alpha) & 0 \\ 0 & 0 & 1 \end{bmatrix}
\begin{Bmatrix} \bar{u}_i \\ \bar{v}_i \\ \bar{\theta}_i \end{Bmatrix}
\Rightarrow
\begin{Bmatrix} \bar{u}_i \\ \bar{v}_i \\ \bar{\theta}_i \end{Bmatrix}
=
\begin{bmatrix} \cos(\alpha) & \sin(\alpha) & 0 \\ -\sin(\alpha) & \cos(\alpha) & 0 \\ 0 & 0 & 1 \end{bmatrix}
\begin{Bmatrix} u_i \\ v_i \\ \theta_i \end{Bmatrix}
\qquad (22)
$$

; As shown in **Fig. 18**-(c), u_i and v_i are the axial and transverse displacement of the i-th node in the global coordinate, and $\bar{u}_i$ and $\bar{v}_i$ are the axial and the transverse displacement corresponding to the local coordinate, respectively. Each node has axial, transverse and rotational DOFs. Thus, the transform matrix can be obtained by:
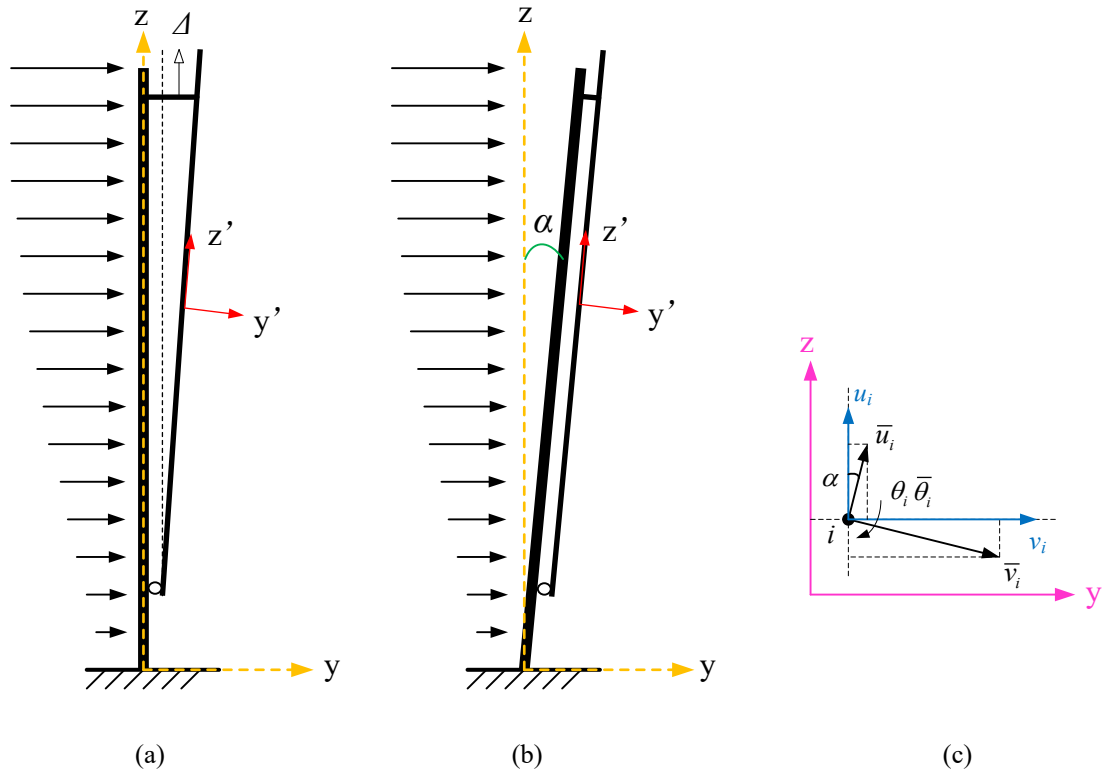
Fig. 18. Conditions for analysis (a) with initial displacement of the liners; (b) with a small rotational angle of the chimney at the base. (c) Coordinate transformation.

With the above relationship between the global and the local coordinates, we take $\Delta = 0.1$ m and $\alpha = 10$ ° as case studies, and we assume that eccentricities do not affect the stiffness and damping of the equivalent tuning system. The results considering the two conditions are shown in **Table 6** and **Table 7**, respectively, indicating that the impact of the unintentional eccentricities on the dynamic response of the tuned chimney is insignificant.

Table 6. Performance of the tuned chimney with and without an eccentricity of the liners.

Wind	Δ (m)	$u_{t,\mathrm{rms}}^{top}$ (m)	$a_{t,\mathrm{rms}}^{top}$ (m/s^2)	$u_{RD,\mathrm{max}}$ (m)
1	0.0	0.187	0.684	0.948
	0.1	0.187	0.684	0.961
2	0.0	0.171	0.644	0.815
	0.1	0.171	0.644	0.912
3	0.0	0.152	0.604	0.740
	0.1	0.152	0.604	0.828
4	0.0	0.190	0.753	0.998
	0.1	0.190	0.753	1.070

Table 7. Performance of the tuned chimney with and without a small rotation of the chimney at the base.

Wind	α (deg)	$u_{t,\mathrm{rms}}^{top}$ (m)	$a_{t,\mathrm{rms}}^{top}$ (m/s^2)	$u_{RD,\max}$ (m)
1	0	0.187	0.684	0.948
	10	0.185	0.672	0.949
2	0	0.171	0.644	0.815
	10	0.169	0.634	0.820
3	0	0.152	0.604	0.740
	10	0.150	0.598	0.742
4	0	0.190	0.753	0.998
	10	0.188	0.743	1.006

7 Conclusions

This paper proposes a novel method to control the along-wind response of high-rise chimneys by coupling and tuning the vibration of the liners to the outer cylinder. A simplified numerical model of the chimney with liners is also proposed and validated against a detailed shell-like FE model of the structure. A design method for chimneys with tuned liners considering along-wind actions is introduced to optimize the response of the tuned structure. The dynamic analysis of a typical high-rise chimney under realistic turbulent wind actions shows the efficiency of the proposed controlling solution. Comparison between the TMD and the proposed solutions further illustrates the advantage of the proposed chimney. The effectiveness of the tuned chimney in the perpendicular direction is also observed and the safety of its operation is demonstrated.

The main conclusions are as follows:

（1）The proposed simplified numerical model of chimney with liners can reflect the structural dynamic characteristics and can be applied to the numerical analysis in the linear elastic range.

（2）The proposed design process is able to obtain suitable parameters for the properties of the tuned structure to achieve the performance requirements in terms of the mitigation effect of absolute vibration and the control of relative vibration under turbulent wind actions.

（3）The proposed method of tuned liners reduces effectively the top displacement (with an average mitigation ratio $\bar{\eta}_{top}$ of about 62%) and the top acceleration (with an average mitigation ratio $\bar{\gamma}_{top}$ of about 70%) of the outer cylinder under along-wind actions. This comes at the expense of increasing the relative displacements of the outer cylinder and the liners, which are however within the required limit. Besides, the proposed solution can be effective in multiple directions.

（4）A control solution with a traditional TMD would require an additional mass of approximately 300 tons to achieve the same response reduction as with the coupled liners, which may be seen as an advantage of the latter.

The proposed methodology to optimize the tuning properties between the liners and the concrete wall is conceived and validated for turbulent wind actions only. Further works should consider the detailed across-flow movements induced by vortex shedding.Preliminary analysis conducted by the authors on the seismic response of the structure with the proposed liner tuning method suggests that it can also be efficient subject to ground motions, but this is being the object of further work. Moreover, dynamic response analysis of the tuned scheme without considering the P-Delta effect is a limitation of the work that is the object of further research.

Acknowledgement

References

[1]   D. Menon. Estimation of along-wind moment in RC chimneys. Engineering Structures, 1997, 19(1): 71-78.

[2]   J. L. Wilson. Earthquake response of tall reinforced concrete chimneys. Engineering Structures, 2003, 25(1): 11-

24.

[3] Y. G. Zheng, J. W. Huang, Y. H. Sun, and J. Q. Sun. Building vibration control by active mass damper with delayed acceleration feedback: Multi-objective optimal design and experimental validation. Journal of Vibration and Acoustics. 2018, 140(4): 041002.

[4] G. Hirsch, H. Ruscheweyh. Full-scale measurements on steel chimney stacks. Journal of Wind Engineering and Industrial Aerodynamics, 1975, 1(4):341-347.

[5] M. Pešata, L. Procházka, J. Boháčová, J. Daňková. Damage of industrial reinforced concrete chimneys caused by high temperatures. Key Engineering Materials, 2019, 4846: 153-158.

[6] S. Elias, V. Matsagar, T. K. Datta. Along-wind response control of chimneys with distributed multiple tuned mass dampers. Structural Control and Health Monitoring, 2019, 26(1): e2275.

[7] J. M. W. Brownjohn, E. P. Carden, C. R. Goddard, G. Oudin. Real-time performance monitoring of tuned mass damper system for a 183m reinforced concrete chimney. Journal of Wind Engineering and Industrial Aerodynamics, 2009, 98(3): 169-179.

[8] F. Telch, G. Lacidogna, O. Rösch. Structural stability assessment of a masonry chimney subjected to shocks by vibration measurements. International Journal of Architectural Engineering Technology, 2018, 5: 38-51.

[9] P. Górski. Dynamic characteristic of tall industrial chimney estimated from GPS measurement and frequency domain decomposition. Engineering Structures, 2017, 148: 277-292.

[10] H. Dosanjh, D. J. Johns. Response to wind of a model chimney with added damping. Earthquake Engineering & Structural Dynamics, 1984, 12(3): 427-430.

[11] P. Gorski, T. Chmielewski. A comparative study of along and cross-wind responses of a tall chimney with and without flexibility of soil. Wind and Structures, 2008, 11(2): 121-135.

[12] P. Gorski. Some aspects of the dynamic cross-wind response of tall industrial chimney. Wind and Structures, 2009, 12(3): 259-279.

[13] Y. F. Xu. The stress performance analysis of chimney structure based on finite element method. Advanced Materials Research, 2014, 3470: 952-956.

[14] S. Elias, R. Rupakhety, S. Olafsson. Tuned mass dampers for response reduction of a reinforced concrete chimney under near-fault pulse-like ground motions. Frontiers in Built Environment, 2020, 6: 92-100.

[15] L. Zhang, S. T. Xue, R. F. Zhang, L. Y. Xie, L. F. Hao. Simplified multimode control of seismic response of high-rise chimneys using distributed tuned mass inerter systems (TMIS). Engineering Structures, 2021, 228: 111550.

[16] Y. K. Qiu, C. D. Zhou, A. Siha. Correlation between earthquake intensity parameters and damage indices of high-rise RC chimneys. Soil Dynamics and Earthquake Engineering, 2020, 137:106282.

[17] C. D. Zhou, M. W. Tian, K. P. Guo. Seismic partitioned fragility analysis for high-rise RC chimney considering multidimensional ground motion. The Structural Design of Tall and Special Buildings, 2019, 28(1): e1568.

[18] Z. Karaca, E. Türkeli, M. Günaydın; S. Adanur. Dynamic responses of industrial reinforced concrete chimneys strengthened with fiber‑reinforced polymers. The Structural Design of Tall and Special Buildings, 2015, 24(3) :228-241.

[19] X. S. Cheng, H. J. Qian, C. Wang, X. D. Fu. Seismic response and safety assessment of an existing concrete chimney under wind load. Shock and Vibration, 2018, 2018(12): 1-12.

[20] N. Longarini, M. Zucca. A chimney's seismic assessment by a tuned mass damper. Engineering Structures, 2014, 79(15): 290-296.

[21] K. S. Dai, C. Fang, S. H. Zhang, Y. F. Shi. Conceptual design and numerical study on a cable-based energy dissipating system for the vibration control reduction of tower-like structures. Engineering Structures, 2021, 237: 112034.

[22] Z. Zhao, K. S. Dai, E. R. Lalonde, J. Y. Meng, B. W. Li, Z. B. Ding, G. Bitsuamlak. Studies on application of scissor-jack braced viscous damper system in wind turbines under seismic and wind loads. Engineering Structures, 2019, 196: 109284.

[23] M. Morga, G. C. Marano. Optimization criteria of TMD to reduce vibrations generated by the wind in a slender structure. Journal of Vibration and Control, 2014, 20(16): 2404-2416.

[24] S. Elias, V. Matsagar, T. K. Datta. Distributed multiple tuned mass dampers for wind response control of chimney with flexible foundation. Procedia Engineering, 2017, 199: 1641-1646.

[25] GB 50135-2019. Standard for design of high-rising structures. China: Ministry of Housing and Urban-Rural Development of the People's Republic of China, 2019.

[26] H. Carvlho, G. Queisoz, P. M. L. Vilela, R. H. Fakury. Dynamic analysis of a concrete chimney considering the aerodynamic damping. IBRACON Structures and Materials Journal, 2019, 12(2): 308-328.

[27] Abaqus/CAE. Version 2020. Dassault Systemes SIMULIA. Paris, France.

[28] H. Aboshosha, A. Elshaer, G. T. Bitsuamlak, A. E. Damatty. Consistent inflow turbulence generator for LES evaluation of wind-induced responses for tall buildings. Journal of Wind Engineering and Industrial Aerodynamics, 2015, 142: 198-216.

[29] ASCE 7-16. Minimum design loads and associated criteria for buildings and other structures. America: The American Society of Civil Engineering, 2016.

[30] Matrix Laboratory (MATLAB). Version 2020a. MathWorks. Natick, Massachusetts, USA.

[31] PEER. PEER ground motion database. Pacific Earthquake Engineering Research Center 2021.